Polymer Bulletin (2024) 81:5215–5235
https://doi.org/10.1007/s00289-023-04963-7

ORIGINAL PAPER

Gelatin-based hydrogels and ferrogels as smart drug delivery systems: synthesis, characterization and drug release kinetics

Deniz Akın Şahbaz[1]

Received: 25 August 2022 / Revised: 13 May 2023 / Accepted: 13 August 2023 /
Published online: 23 August 2023

Abstract

The objective of this study was to develop biodegradable, environmentally friendly, economical and smart gelatin-based hydrogels and ferrogels as controlled drug delivery systems. Cross-linking is an important treatment for controlling the drug release from hydrogels, as well as enhancing the thermal and mechanical stability of hydrogels. In this study, gelatin-based hydrogels and ferrogels were synthesized at different cross-linker concentrations, ranging from 4 to 16 wt% to allow for different mesh and pore sizes in the gelatin matrix. The gels were characterized by thermogravimetric analysis, Fourier transform infrared spectroscopy, scanning electron microscopy, and energy dispersive X-ray spectroscopy. The swelling properties and in-vitro release of tetracycline as a model drug from the hydrogels and ferrogels cross-linked with different ratios by the diffusion mechanism were tested in solutions of pH 6.5 and 7.4 at 37 °C, which mimics environments similar to those of the mouth and intestines. The results showed that the swelling and drug release properties of all the gelatin hydrogels and ferrogels significantly depended on the cross-link level because of the effect of the cross-linking mechanism on reducing the number of free carboxyl and free amino groups of gelatin matrix. In addition, it was observed that the presence of magnetic nanoparticles in the gelatin matrix has an effect of decreasing the swelling and drug release percent of the gelatin-based hydrogels.

✉ Deniz Akın Şahbaz
dsahbaz@pau.edu.tr

[1] Department of Chemical Engineering, Faculty of Engineering, Pamukkale University, 20070 Kınıklı, Denizli, Turkey

Graphical abstract

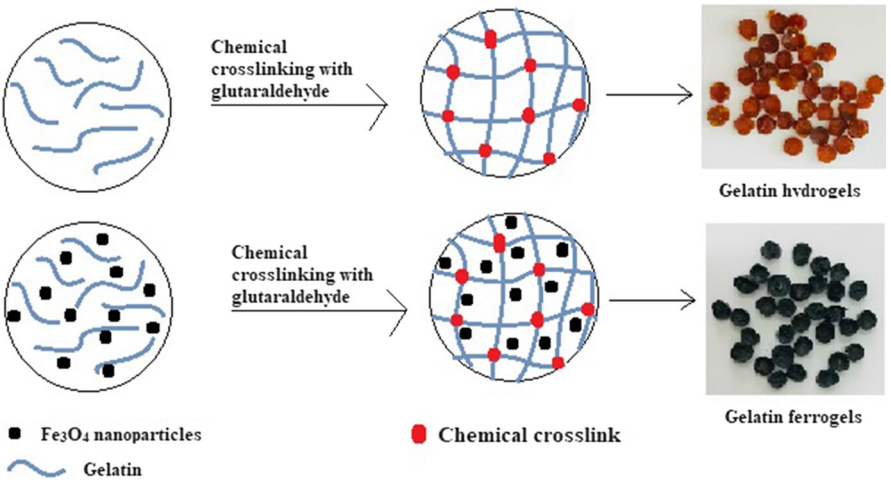

Keywords Hydrogel · Gelatin · Ferrogel · Drug release · Kinetics · Cross-linking

Introduction

Controlled release is described as a process in which one or more active agents are intended to come out of a system at a desirable site, time and at a definite rate. In recent years, studies on controlled drug release systems that can reach certain one or more regions of the living organism and control the release rate of the trapped drug have increased in biomaterials and biomedical applications. In the selection of drug carrier materials for controlled drug release systems, natural and synthetic biomedical polymers such as chitosan [1], cellulose [2], gelatin [3–7], polyvinyl alcohol [8], polyacrylic acid [9], polyethylene glycol [10, 11] are generally preferred due to their biocompatibility, biodegradability, nontoxicity, and antibacterial properties.

Hydrogels are attracting increased attention lately because of their potential in drug delivery systems. They are polymeric structures that have the properties of gelation, functionalization, being hydrophilic, having three-dimensional meshes that are capable of absorbing large amounts of water or biological fluids, and swelling without dissolving in water [12–14]. However, they are not efficient enough for targeting and holding drug molecules at the specific site in the body. Magnetic nanoparticles are considered as one of the most effective solutions to these problems. The magnetic nanoparticles could easily isolate in the targeted area under an external magnetic field, and also be introduced into a polymeric matrix or coated with polymers, so that the magnetic nanoparticles have potential application in drug targeting and drug delivery as drug carriers [15, 16]. Recently, natural polymer hydrogels functionalized with magnetic materials (or called ferrogels) are receiving increasing attention as intelligent drug delivery

devices because of their rapid response, selective targeting, and also remote controllability [17]. Several biopolymers such as alginate [18–20], chitosan [21], κ-carrageenan [22], agarose [23] have been used for preparation of ferrogels as efficient drug carriers for delivering various types of drugs.

Among these biopolymers, gelatin, which is derived from collagen, has received extensive attention in the preparation of ferrogels due to its superior physicochemical features, antioxidant activity, acceptable biocompatibility, biodegradability, antimicrobial properties, gelation ability, better film-forming characteristics and relatively low cost [24]. These features make gelatin-based hydrogels remarkable for tissue engineering [25], drug delivery [26], magnetic resonance imaging [27], wastewater treatment [28], hyperthermia cancer therapy [29] applications.

However, gelatin-based hydrogels have poor mechanical strength, and formation of cracks in polymeric networks leads to a relatively fast degradation rate. The problem can be solved by a chemically, enzymatically or physically cross-linking process as well as formulation of hybrid gelatin-based hydrogels with metal nanoparticles and metal oxide [21, 30]. Physical cross-linking of hydrogels is carried out by cooling the solution of gelatin below 35 °C to partial recovery of the triple-helix structure of collagen. However, hydrogels have low mechanical and chemical stability above 35 °C because of the breaking of the secondary bonding structure [31, 32]. Gelatin can be easily chemically cross-linked with cross-linkers due to accessible functional groups such as amine, carboxyl and hydroxyl [15]. The chemical cross-linking of gelatin not only improves its physicochemical properties, but also enhances its mechanical properties. The cross-linking mechanism also affects its drug release mechanism as well as physicochemical properties.

In literature studies, there are numerous research that have investigated the applications of cross-linked gelatin-based hydrogels as drug delivery systems for nucleic acid [33], antibacterial [34], anticancer [35, 36], and anti-inflammatory drugs [37]. Some studies have also showed the influence of the chemical cross-linking method [38], cross-linking agent type [39], embedding of drug-loaded nanoparticles into the hydrogel structure [40], water content [41], polymer and monomer ratios [42], drug loading technique [43] on the characteristics of gelatin-based composites and/or their drug release profiles. However, the effect of cross-linking amounts in gelatin ferrogels and hydrogels on the drug release mechanism and kinetics has not been reported previously.

In the present study, it was aimed at synthesizing gelatin-based hydrogels and ferrogels as efficient and smart drug delivery systems in the presence of different ratios of cross-linking agents to raise the mechanical properties and structural integrity of polymer matrix. This research study also emphasizes kinetic models of in-vitro drug release to understand the mechanism of drug release from drug-loaded hydrogels and ferrogels. In addition, swelling studies of the fabricated hydrogels in pH 6.5 and 7.4 media were assessed systematically. The gels were characterized by thermogravimetric analysis (TGA), Fourier transform infrared (FTIR) spectroscopy, scanning electron microscopy (SEM), and energy dispersive X-ray (EDX) spectroscopy to evaluate the interaction of the gelatin and cross-linker.

Materials and methods

Materials

Gelatin (from bovine skin) used as a polymer in the synthesis of hydrogels and ferrogels and glutaraldehyde solution ($OHC(CH_2)_3CHO$, 50%) used as cross-linker were purchased from Sigma-Aldrich company. Tetracycline ($C_{22}H_{24}N_2O_8.xH_2O$) used as a drug active agent was obtained from Merck company. In the synthesis of Fe_3O_4 nanoparticles, which have been used to gain magnetic properties of hydrogels, iron(III) chloride hexahydrate ($FeCl_3.6\ H_2O$, 97% Sigma-Aldrich), iron(II) chloride tetrahydrate ($FeCl_2.4H_2O$, 99%, Sigma-Aldrich) and ammonia solution (NH_4OH, 25%, Merck) was used. Phosphate Buffer Solution (PBS, Sigma-Aldrich) was used to determine both swelling properties and drug release behavior of synthesized hydrogels and ferrogels.

Synthesis of Fe_3O_4 nanoparticles

A co-precipitation method was used in the synthesis of magnetic Fe_3O_4 nanoparticles as described in our previous study [44, 45]. In this method, magnetic Fe_3O_4 nanoparticles were synthesized based on a stoichiometric mixture of $FeCl_2.4H_2O$ and $FeCl_3.6H_2O$ reactive salts with a molar ratio of 3:2 under the aqueous ammonia (%25 v/v) as the precipitating agent. The synthesis of Fe_3O_4 nanoparticles in alkaline medium is shown in Fig. 1.

The synthesis process was carried out under inert atmosphere to prevent oxidation of Fe^{2+} and Fe^{3+} salts and possible side reactions. A mixture of $FeCl_2{\cdot}4H_2O$ and $FeCl_3{\cdot}6H_2O$ was introduced to 150 mL of deionized water. The mixture was stirred with a mechanical stirrer (RZR 2021, Heidolph) at 90 °C for 1 h. Then, ammonia solution (25% v/v) was added dropwise to the system with a peristaltic pump within 30 min. The brown-colored Fe_3O_4 nanoparticles were collected using a magnetic field by a permanent magnet, washed using distilled water until the pH value descended to 7.0, and dried at room temperature.

Synthesis of gelatin-based hydrogels and ferrogels

Gelatin hydrogels and ferrogels were synthesized using a solvent casting method [26, 46] at different cross-linker concentrations, ranging from 4 to 16 wt% to allow for different mesh and pore sizes in the gelatin gels. In detail, the gelatin solutions (10 wt%) were prepared by mixing gelatin in deionized water at 40 °C using a magnetic stirrer. After the gelatin powder was fully dissolved, glutaraldehyde solutions at different concentrations (4, 8, 12, and 16 wt%) were added dropwise to the gelatin solutions under stirring, and stirred for further 5 min. After the gelation was performed, the mixtures were poured onto cylindrical tubes, followed by air-drying at room temperature for 24 h to allow the solidification. Subsequently, the resultant gelatin hydrogels were peeled out from the cylindrical tubes. The hydrogels were

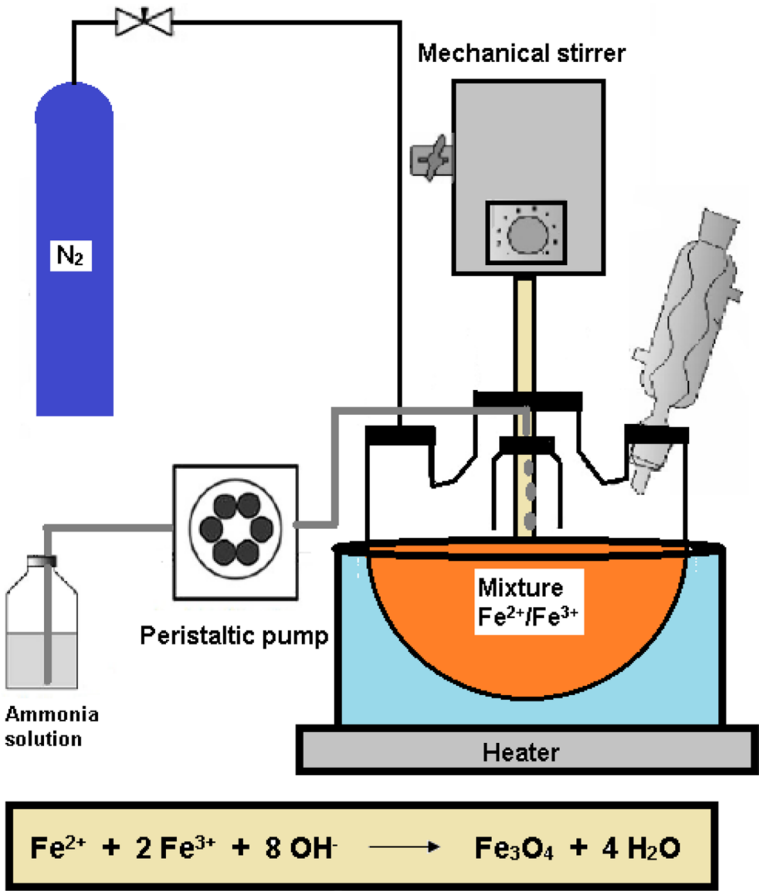

Fig. 1 Shematic representation for the synthesis of Fe_3O_4 nanoparticles

then washed multiple times with deionized water to remove the unreacted residues and cut into 10 mm discs followed by freeze-driering using a lyophilizer at − 80 °C for 24 h. The hydrogels were designated as GH4, GH8, GH12, and GH16 according to their different cross-link densities, which indicates the glutaraldehyde content is 4, 8, 12, and 16 wt%, respectively.

A two-step process was applied to prepare the gelatin ferrogels. In the first step, magnetic Fe_3O_4 nanoparticles were prepared using a co-precipitation method. Second, the magnetic nanoparticles were added in a 10% (w/w) ratio to the gelatin solutions. Then, the resulting black color mixture was homogenized for 10 min using an ultrasonic bath. Finally, the cross-linking, washing, and freeze-drying methods similar to procedures in the preparation of gelatin hydrogel samples as described above were used to obtain the gelatin ferrogels. The ferrogels were designated as GF4, GF8, GF12, and GF16 according to their different cross-link densities, which indicates the glutaraldehyde content is 4, 8, 12, and 16 wt%, respectively.

Drug loading of gelatin-based hydrogels and ferrogels

One of the general methods for drug loading of hydrogels as drug carriers is to incorporate a drug into the system during the synthesis of hydrogels [47, 48]. In this study, tetracycline as a model drug was added to the gelatin solution at a concentration of 5 wt%. In the synthesis process of the gelatin hydrogels and ferrogels, the gelatin monomer is allowed to polymerize with glutaraldehyde solution used as a cross-linker and the tetracycline molecules get trapped inside the polymer structure.

Characterization of gelatin-based hydrogels and ferrogels

Morphology of the hydrogels and ferrogels was observed using Scanning Electron Microscopy (SEM). The samples were mounted on brass pins and were sputter-coated with gold in a sputter coater. They were then visualized using SEM (LEO, 1430 VP, Carl Zeiss, Germany) operated at an acceleration voltage of 20 kV at varying magnifications. The mapping images of iron and chemical composition were taken by SEM equipped with energy dispersive X-ray spectroscopy (EDX). The chemical structure of hydrogels and ferrogels were investigated by Fourier transform infrared spectroscopy (FTIR, Thermo Scientific, NICOLET iS50FT-IR) equipped with an ATR assembly. All spectra were the average of 32 scans in the range of 4000–400 cm^{-1} with a spectral resolution of 4 cm^{-1}. The thermal behavior of the gelatin hydrogels and ferrogels was measured by a simultaneous thermal analyzer (STA, NETZSCH, STA 449 F3 Jupiter) operating at a heating rate of 10 °C/min from 25 to 600 °C under nitrogen (N_2) gas.

Swelling of the gelatin-based hydrogels and ferrogels

Gravimetric methods were used for determining the swelling percentage of the prepared hydrogels and ferrogels [49]. Firstly, the freeze-dried hydrogel and ferrogel samples were weighed (W_d) and immersed in solutions of pH 6.5 and 7.4 at 37 °C, which mimics environments similar to those of the mouth and intestines. Then, at different time intervals, the samples were removed from the swelling medium and weighed (W_s) after the excess fluid on the surface was absorbed with a filter paper. The changes in weight of the swollen hydrogels were regularly observed and the process was repeated until a weight change between two readings was constant. All tests were performed in triplicate.

The swelling ratio for each hydrogel and ferrogel was calculated using Eq. (1):

$$Swelling\% = \frac{W_s - W_d}{W_d} \times 100 \tag{1}$$

where W_s represents the weight of the swollen sample and W_d is the initial weight of freeze-dried hydrogel samples, respectively.

In-vitro drug release studies

Gelatin hydrogels and ferrogels were added to a 50 mL plastic tube with 30 mL of different PBS solutions (pH = 5.0 and pH = 7.4) and then stirred at 100 rpm at 37 °C. After certain time, 1 mL samples of the each drug release solutions were collected from the tubes with replacement of an equal volume of the fresh solution and then the collected samples were analyzed at 360 nm using a UV–vis spectrometer (Shimadzu, UVmini-1240). The release experiments were carried out by triplicate. The drug release percent was determined according to the following Eq. (2) [47]:

$$Drug\ release\ (\%) = \frac{M_t}{M_\infty} \times 100 \tag{2}$$

where M_∞ and M_t represent the initial amount of drug-loaded and the cumulative amount of drug released at the time t.

Results and discussion

Morphological and structural analysis

The surface morphologies of the cross-linked gelatin hydrogels and ferrogels were investigated using SEM. When the SEM micrographs in Fig. 2 are examined, it is seen that both hydrogels and ferrogels have a porous structure by virtue of the freeze-drying step with the pores being the result of ice crystal formation [50], but the ferrogels have uneven surface and formed rough protrusions. This phenomenon can originate from the incorporation of Fe_3O_4 nanoparticles in the gelatin matrix, resulting in a slightly irregular surface of the ferrogels. Similar results were also observed by other researchers. Zeng et al. [51] have reported that higher Fe_3O_4 nanoparticles content causes a rough surface on the pore wall of magnetic hydrogels. Similarly, Li et al. [52] have shown that the surface of pure hydrogels is smooth and flat, while the surface of magnetic hydrogels is irregular and rough.

Moreover, the elemental composition of Fe in the magnetic hydrogels was analyzed by SEM/EDX analysis. The SEM images of the ferrogels demonstrate that the Fe_3O_4 nanoparticles are fairly uniformly distributed in the gelatin matrix. The homogeneous distribution of the Fe_3O_4 nanoparticles in the ferrogel was confirmed by EDX mapping and the blue dots represent Fe in the gelatin gel in Fig. 3.

Figure 4 shows the EDX pattern of gelatin hydrogel and ferrogels. The presence of carbon, oxygen, and nitrogen is attributed to gelatin. The signals for iron in Fig. 4b confirm the existence of iron oxide nanoparticles within the ferrogel network. The peaks at 1.75 to 2.25 keV are related to gold, which was used for sample coating. The detected weight and atomic fractions of carbon, oxygen, nitrogen, and iron elements are given in Table 1. According to the EDX findings, the amount of Fe in the gelatin ferrogel sample was calculated as 5.74 (wt%).

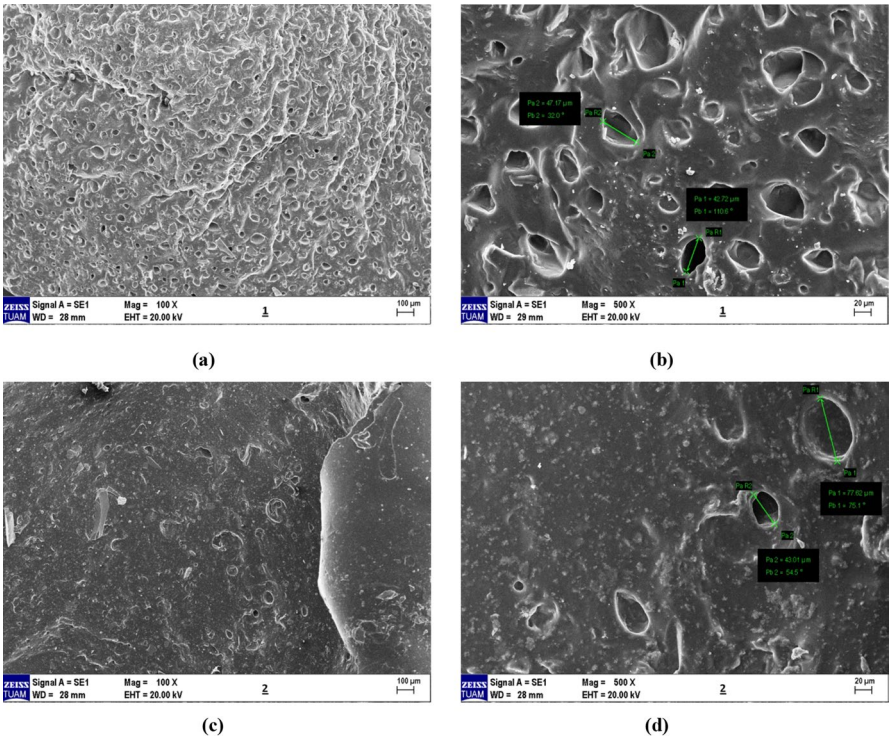

(a) **(b)** **(c)** **(d)**

Fig. 2 SEM images of gelatin hydrogels (**a**, **b**) and ferrogels (**c**, **d**)

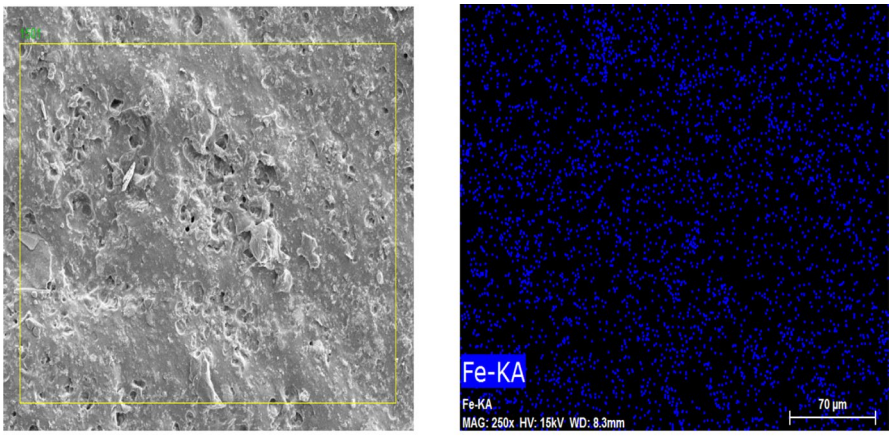

(a) **(b)**

Fig. 3 SEM image of cross-section of gelatin ferrogel **a** and EDX mapping of iron (blue signal) in the image (scale bar: 70 µm) **b**

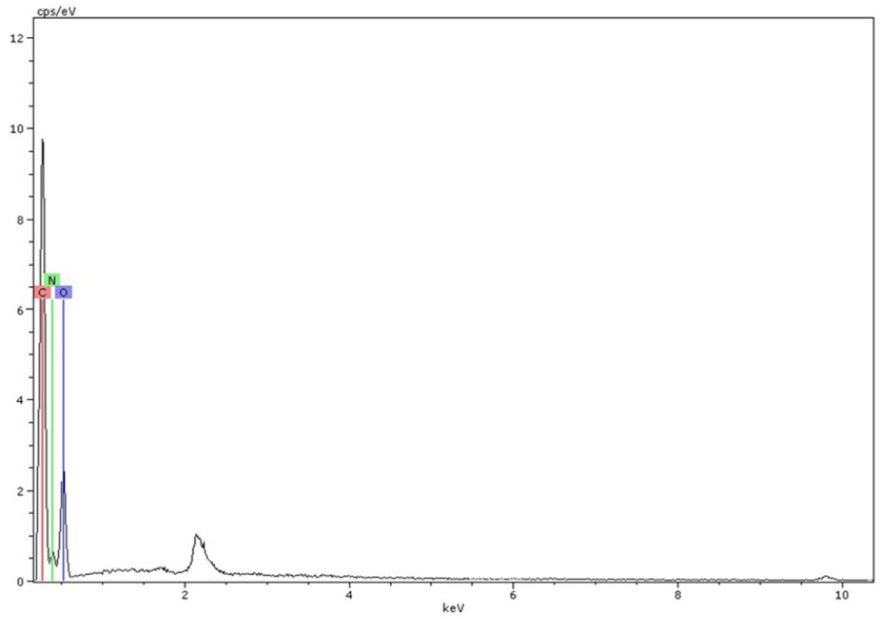

(a)

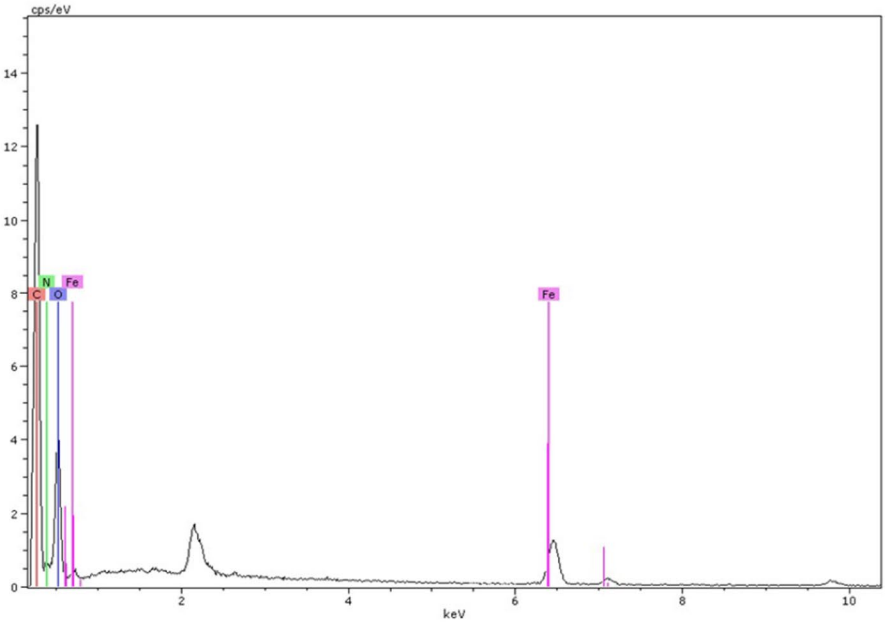

(b)

Fig. 4 EDX analysis of gelatin hydrogel **a** and ferrogel **b**

Table 1 Results of the EDX analysis of the gelatin hydrogels and ferrogels

Element	Gelatin hydrogels		Gelatin ferrogels	
	Weight %	Atomic %	Weight %	Atomic %
Oxygen	47.66	41.80	47.33	43.47
Carbon	34.66	40.49	33.05	40.45
Nitrogen	17.68	17.71	13.88	14.57
Iron	–	–	5.74	1.51
Total	100.00	100.00	100.00	100.00

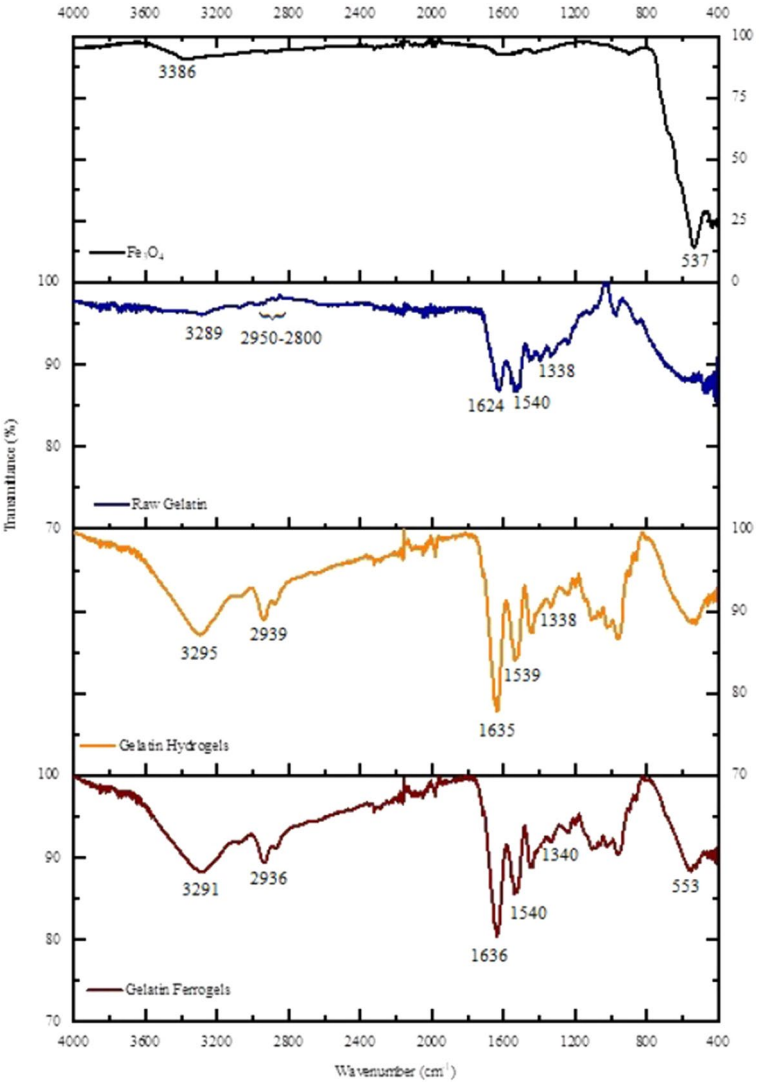

Fig. 5 FTIR spectra of Fe_3O_4 **a**, raw gelatin **b**, gelatin hydrogels **c** and gelatin ferrogels **d**

The FTIR spectra of Fe_3O_4, raw gelatin, gelatin hydrogels and ferrogels are presented in Fig. 5. In all the samples, the broad peak in the range of 3200–3600 cm^{-1} is related to O–H stretching vibrations [53]. Amide groups of gelatin peptide bonds exhibit characteristic absorption spectral peaks in specific bands, which are amide I (1600–1800 cm^{-1}), II (1470–1570 cm^{-1}), and III (1250–1350 cm^{-1}) bands [54]. All these characteristic bands are present in the spectrum for raw gelatin, gelatin hydrogels and ferrogels too. The other characteristic band which corresponds to the C–H stretching is observed at the range 2800–2950 cm^{-1} [15]. The FTIR spectrum of Fe_3O_4 shows a peak at 537 cm^{-1} which corresponds to vibrations of the Fe–O bonds [55]. The characteristic peak is observed in the spectrum for gelatin ferrogels too.

Thermal stability

Thermal stability is one of the most important properties related to the cross-linking density of the hydrogels. Therefore, thermogravimetric analysis (TGA) was carried out to investigate the thermal properties of the gelatin hydrogels and ferrogels cross-linked with different weight ratios of cross-linkers. As shown in Fig. 6, all the gelatin hydrogels and ferrogels showed two steps of weight loss. In detail, the gelatin hydrogels were decomposed with initial weight losses of between 9.6 and 10.9%, attributed to a combination of physical and chemical evaporation of water trapped in the hydrogel matrix at 25 to 200 °C, followed by the second stage observed major weight losses in the temperature range of 200–450 °C due to the degradation of gelatin and polymer chains [56–58]. Weight losses of the GH4, GH8, GH12, and GH16 in the temperature range of 200–450 °C were 77.2%, 76.6%, 71.9%, 57.6%, respectively. In this temperature range, it was observed that hydrogels with a higher cross-linking degree showed lower weight losses than that of hydrogels with a lower cross-linking degree, indicating that cross-linking density has a positive effect on thermal stability. After 450 °C, the loss rate slowed down, and the residue of the GH4, GH8, GH12, and GH16 at 600 °C were calculated as about 1.7%, 3.3%, 11.3%, and 24.3%, respectively. The cross-linked gelatin ferrogels showed a similar degradation process. However, it was observed that the decomposition of the cross-linked gelatin ferrogels in the temperature range of 200–450 °C was quite lower than that of the hydrogels. This phenomenon originated from the incorporation of Fe_3O_4 nanoparticles in the gelatin matrix that enhanced thermal stability of the system due to strong interactions (e.g., hydrogen bonding) between the Fe_3O_4 nanoparticles and the gelatin matrix [15]. As shown in Fig. 6b, magnetite presents high thermal stability and only one step observed weight losses of approximately 8.4% in the temperature range from 25.0 to 600 °C, which is similar to the literature results [59].

Swelling behaviors

Gelatin can swell up and absorb 5–10 times its mass of water to form a gel in aqueous solutions [60]. The swelling properties of gelatin-based hydrogels fabricated by a physical and chemical cross-linking process can be controlled by cross-linking

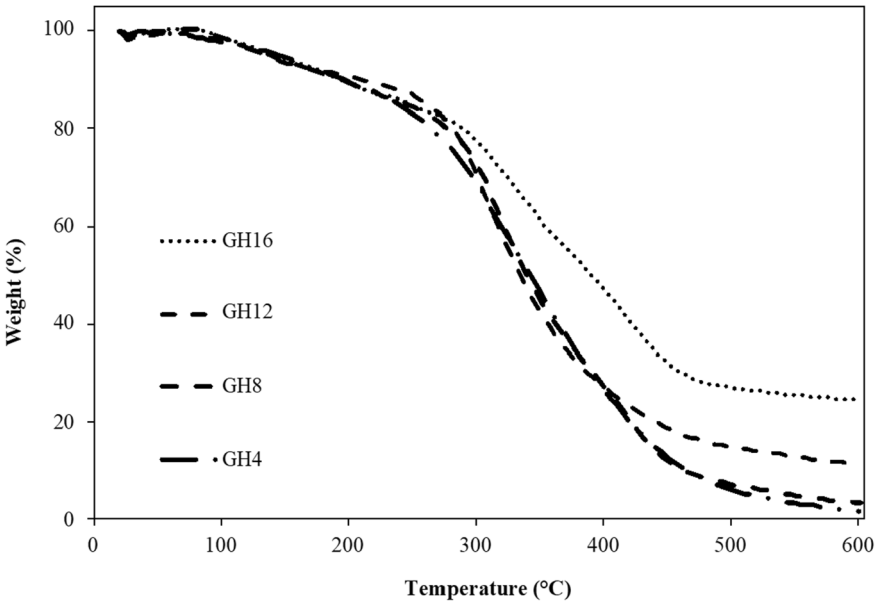

(a)

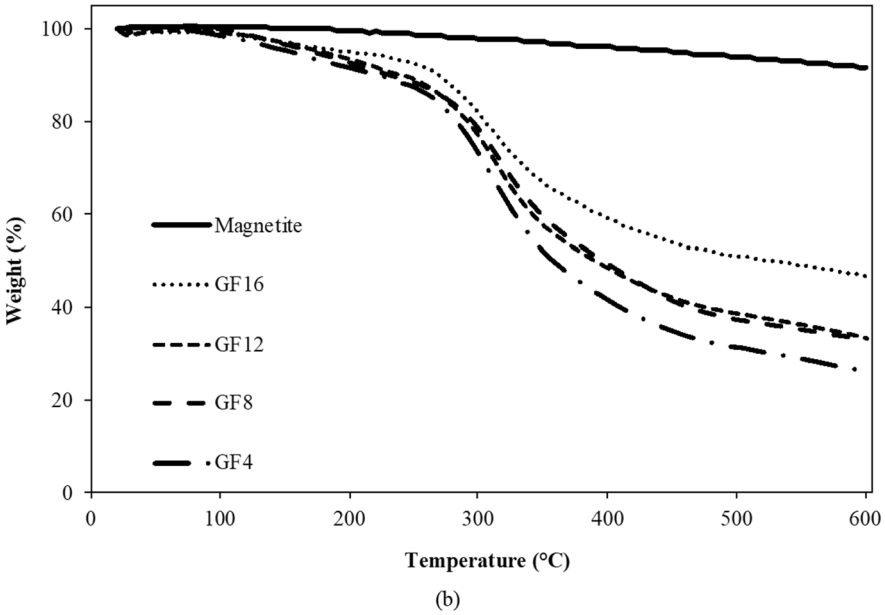

(b)

Fig. 6 Thermal decomposition of **a** gelatin hydrogels (GH4, GH8, GH12, and GH16), **b** magnetite and gelatin ferrogels (GF4, GF8, GF12, and GF16)

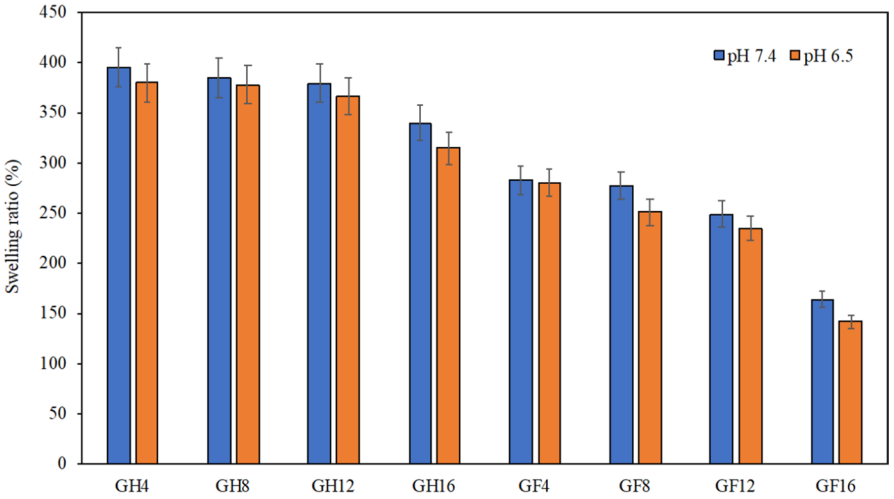

Fig. 7 The swelling ratio of gelatin hydrogels and ferrogels in buffer solutions of pH 6.5 **a** and pH 7.4 **b** at 37 °C

degrees. In this study, swelling behavior of the gelatin hydrogels and ferrogels synthesized at different cross-linker concentrations were studied in buffer solutions of pH 6.5 and 7.4. As shown in Fig. 7, it was observed that the change in the pH of swelling medium from 7.4 to 6.5 did not have much effect on the swelling behavior of the gelatin hydrogels and ferrogels, but the change in glutaraldehyde content had a significant effect on the swelling behavior. The increase in glutaraldehyde content in the samples decreased the overall swelling ratios of the hydrogels and ferrogels, as a result of higher cross-linker proportions. This result is explained by the higher cross-linking densities causing a decrease in solvent uptake and equilibrium swelling ratio [32]. In addition, the gelatin hydrogels at both pH levels (6.5 and 7.4) have higher swelling ratios than those of gelatin ferrogels at the same conditions due to the higher gelatin content. In literature studies, it has been reported that gelatin exhibits good swelling properties due to its hydrophilic groups, such as single bond CO, NH, NH_2 and COO−, providing the diffusion of water molecules through the polymeric matrix [61]. Moreover, the internal network structure of the gelatin ferrogels is tighter than gelatin hydrogels due to the good bonding of gelatin molecules with nano F_3O_4 nanoparticles as coordination bonds, which reduces the swelling ratio of hydrogels.

Drug release kinetics

The tetracycline release from the hydrogels and ferrogels was tested in solutions of pH 6.5 and 7.4 at 37 °C, which mimics environments similar to those of the mouth and intestines. As shown in Fig. 8, the cumulative drug release percent of gelatin hydrogels and ferrogels is very high at the beginning. After 8 h, they basically reached the equilibrium of release. The cumulative release percent of gelatin hydrogels (GH4, GH8,

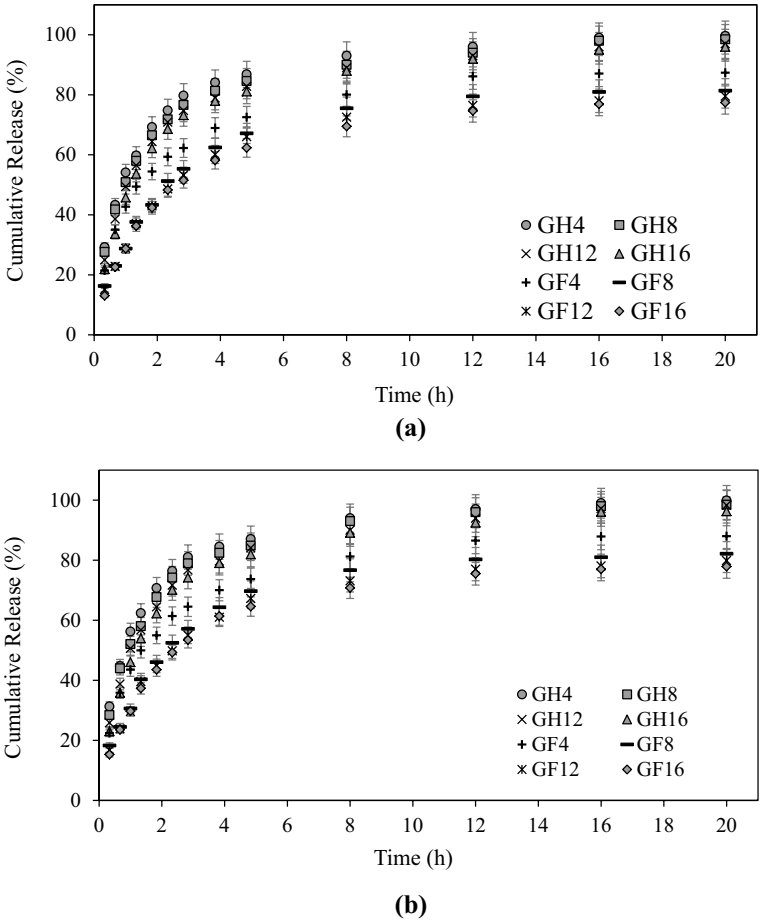

Fig. 8 In-vitro drug release profiles of tetracycline-loaded gelatin hydrogels and ferrogels in solutions of pH 6.5 **a** and pH 7.4 **b** at 37 °C

GH12, and GH16) is much higher than that of ferrogels (GF4, GF8, GF12, and GF16) due to the higher swelling ratio in the hydrogels than ferrogels. The release of drugs from hydrogels and ferrogels involves the absorption of water molecules into the matrix followed by desorption of drug molecules from pores by a diffusion mechanism [47].

To investigate the drug release kinetics and mechanism of the gelatine hydrogels and ferrogels, the drug release data was fitted into various kinetic models such as zero order (Eq. 3), first order (Eqs. 4, 5), Higuchi (Eq. 6), Korsmeyer-Peppas (Eqs. 7, 8) models [62].

Zero Order:

$$M_t = M_0 + k_0 t \tag{3}$$

First Order:

$$M_t = M_0 e^{-k_1 t} \tag{4}$$

$$ln\frac{M_t}{M_0} = k_1 t \tag{5}$$

Higuchi Model:

$$M_t = k_H t^{0.5} \tag{6}$$

Korsmeyer-Peppas model:

$$\frac{M_t}{M_\infty} = k_K t^n \tag{7}$$

$$ln\frac{M_t}{M_\infty} = \ln k_K + n \ln t \tag{8}$$

where M_t and M_∞ represent the amount of released active agent at time t and infinite time, respectively. M_0 is the initial amount of the active agent in the solution (most times, $M_0 = 0$). k_0 and k_1 are the zero order and the first order release constants, respectively. k_H is the Higuchi constant of dissolution and k_K is the Korsmeyer-Peppas model rate constant, which reveals structural and geometric character of the drug release matrix. M_t/M_∞ is the fraction of released tetracycline until time t, n is the release diffusional exponent incorporating the mechanism of the drug release.

The experimental release data were evaluated by plotting the cumulative % drug release versus time for the zero-order kinetic model; log cumulative % drug remaining vs time for the first-order kinetic model; cumulative % drug release vs square root of time for the Higuchi model; log cumulative % drug release versus log time for the Korsmeyer–Peppas model [63].

Correlation coefficient (R^2) values that were used to evaluate the predictive accuracy of the kinetic models are given in Table 2. By comparing the calculated R^2 values for the four release kinetic models, it was observed that the release kinetics best fitted with the Korsmeyer-Peppas model for all hydrogels and ferrogels. The R^2 values ranged from 0.9837 to 0.9979 in both mediums (pH 7.4 and 6.5), indicating that the tetracycline release mechanism of the hydrogels and ferrogels follows the Korsmeyer–Peppas kinetic model. The values of n evaluated for the slopes of the curves are used to determine the type of drug diffusion from developed hydrogels. n value is in the range of 0.45–0.5 and 0.5–0.89 refers to Fickian (diffusion-controlled) and non-Fickian (diffusion and erosion-controlled) release, respectively. If n is between 0.89 and 1.0, it corresponds to case II (zero-order) transport. If n value is above 1.0, the phenomenon corresponds to super Case II transport [20, 64, 65]. As can be seen from Table 2, the values of n determined for all hydrogels and ferrogels are in the range of 0.5080 to 0.6558, which corresponds to a non-Fickian diffusion and erosion controlled release mechanism. Similar results were reported for the release of other drugs from the polymeric hydrogels: ibuprofen [20], (±)-2-(p-isobutylphenyl)propionic acid [66], and cyclophosphamide anticancer drug [67]. When the drug release

Table 2 Tetracycline release kinetic parameters for the gelatin hydrogels and ferrogels at pH 6.5 and 7.4

Hydrogel identification	pH	Correlation Coefficient (R^2)					
		Zero order	First order	Higuchi model	Korsmeyer–Peppas model	Release exponent 'n' from Korsmeyer–Peppas model	Rate constant K_K from Korsmeyer model
GH4	6.5	0.5990	0.4661	0.7771	0.9941	0.5271	0.5277
	7.4	0.5919	0.4749	0.7707	0.9967	0.5080	0.5492
GH8	6.5	0.6269	0.4843	0.8006	0.9960	0.5367	0.5056
	7.4	0.6064	0.4723	0.7845	0.9851	0.5193	0.5162
GH12	6.5	0.6215	0.4700	0.7961	0.9976	0.5965	0.4854
	7.4	0.6228	0.4749	0.7971	0.9961	0.5796	0.4914
GH16	6.5	0.6194	0.4605	0.7947	0.9979	0.6558	0.4478
	7.4	0.6175	0.4657	0.7937	0.9993	0.6191	0.4567
GF4	6.5	0.6795	0.5159	0.8465	0.9750	0.5193	0.4064
	7.4	0.6686	0.5119	0.8380	0.9807	0.5086	0.4165
GF8	6.5	0.6850	0.5307	0.8520	0.9933	0.5932	0.3023
	7.4	0.6679	0.5251	0.8384	0.9888	0.5572	0.3236
GF12	6.5	0.6896	0.5260	0.8555	0.9957	0.5995	0.2942
	7.4	0.6778	0.5233	0.8457	0.9905	0.5721	0.3102
GF16	6.5	0.6980	0.5100	0.8619	0.9837	0.6133	0.2800
	7.4	0.6769	0.5143	0.8455	0.9943	0.5766	0.2978

rate constants determined according to the Korsmeyer–Peppas model of both hydrogels and ferrogels synthesized with different ratios of cross-linker were compared, it was observed that the increase in the amount of cross-linker decreased the drug release rate. Therefore, all the results show that variations of cross-linker amount can be utilized to control the release percent and rate of drugs from hydrogels and ferrogels according to the necessity of definite applications.

Conclusion

The study is important to show the effect of cross-linking density and Fe_3O_4 addition on the swelling properties and drug release performance of the gelatin-based gels. Firstly, the hydrogels and ferrogels were successfully fabricated by chemically cross-linking using different amounts of glutaraldehyde as a cross-linking agent. Then, the underlying diffusion mechanism of drug release from the hydrogels and ferrogels was investigated using tetracycline as a model drug. The swelling and drug release ratios of the gelatin hydrogels and ferrogels were found to significantly decrease with the increase in the cross-linker ratio in the gelatin matrix, i.e. with the increase in the degree of cross-linking. The cumulative drug release from the gels had maximum stages ranging from 77.9% for GF16 to 99.9% for GH4 at pH 7.4 and maximum stages ranging from 77.4% for GF16 to 99.6% for GH4 at pH 6.5. The results obtained demonstrate clearly that it is possible to control drug release from gelatin-based gels that can be achieved by the variation of the chemical cross-linking level, as a result of the changing structural properties. The study also showed that the combination of gelatin hydrogel and Fe_3O_4 nanoparticles gives a synergistic effect to the newly formed gels. While the remarkable improvements in thermal properties were observed in hydrogel when Fe_3O_4 nanoparticles were inserted in the gelatin matrix, drug release and swelling ratios of the gelatin gels have been significantly decreased.

Declarations

Conflict of interest The author declares there is no conflicts of interest regarding the publication of this paper. The paper has not been published elsewhere and that it has not been submitted simultaneously for publication elsewhere.

References

1. Fonseca-Santos B, Chorilli M (2017) An overview of carboxymethyl derivatives of chitosan: their use as biomaterials and drug delivery systems. Mater Sci Eng C 77:1349–1362. https://doi.org/10.1016/j.msec.2017.03.198
2. Wang R, Shou D, Lv O, Kong Y, Deng L, Shen J (2017) pH-Controlled drug delivery with hybrid aerogel of chitosan, carboxymethyl cellulose and graphene oxide as the carrier. Int J Biol Macromol 103:248–253. https://doi.org/10.1016/j.ijbiomac.2017.05.064

3. Liu TY, Hu SH, Liu KH, Liu DM, Chen SY (2006) Preparation and characterization of smart magnetic hydrogels and its use for drug release. J Magn Magn Mater 304(1):e397–e399. https://doi.org/10.1016/j.jmmm.2006.01.203
4. García-Astrain C, Guaresti O, González K, Santamaria-Echart A, Eceiza A, Corcuera MA, Gabilondo N (2016) Click gelatin hydrogels: Characterization and drug release behaviour. Mater Lett 182:134–137. https://doi.org/10.1016/j.matlet.2016.06.115
5. Biswal D, Anupriya B, Uvanesh K, Anis A, Banerjee I, Pal K (2016) Effect of mechanical and electrical behavior of gelatin hydrogels on drug release and cell proliferation. J Mech Behav Biomed Mater 53:174–186. https://doi.org/10.1016/j.jmbbm.2015.08.017
6. Varghese JS, Chellappa N, Fathima NN (2014) Gelatin–carrageenan hydrogels: role of pore size distribution on drug delivery process. Colloids Surf B Biointerfaces 113:346–351. https://doi.org/10.1016/j.colsurfb.2013.08.049
7. Treesuppharat W, Rojanapanthu P, Siangsanoh C, Manuspiya H, Ummartyotin S (2017) Synthesis and characterization of bacterial cellulose and gelatin-based hydrogel composites for drug-delivery systems. Biotechnol Rep 15:84–91. https://doi.org/10.1016/j.btre.2017.07.002
8. Prabha G, Raj V (2017) Sodium alginate–polyvinyl alcohol–bovin serum albumin coated Fe_3O_4 nanoparticles as anticancer drug delivery vehicle: doxorubicin loading and in vitro release study and cytotoxicity to HepG2 and L02 cells. Mater Sci Eng C 79:410–422. https://doi.org/10.1016/j.msec.2017.04.075
9. Singh B, Sharma V (2017) Crosslinking of poly (vinylpyrrolidone)/acrylic acid with tragacanth gum for hydrogels formation for use in drug delivery applications. Carbohydr Polym 157:185–195. https://doi.org/10.1016/j.carbpol.2016.09.086
10. Wu J, Xie X, Zheng Z, Li G, Wang X, Wang Y (2017) Effect of pH on polyethylene glycol (PEG)-induced silk microsphere formation for drug delivery. Mater Sci Eng C Mater Biol Appl 80:549–557. https://doi.org/10.1016/j.msec.2017.05.072
11. Bubpamala T, Viravaidya-Pasuwat K, Pholpabu P (2020) Injectable poly (ethylene glycol) hydrogels cross-linked by metal–phenolic complex and albumin for controlled drug release. ACS Omega 5:19437–19445. https://doi.org/10.1021/acsomega.0c01393
12. Dreiss CA (2020) Hydrogel design strategies for drug delivery. Curr Opin Colloid Interface Sci 48:1–17. https://doi.org/10.1016/j.cocis.2020.02.001
13. Kwon Y, Song M, Hwang YG, Chang SH, Hong WJ (2008) Effect of materials structure and composition on properties of siloxane-containing hydrogels. Curr Appl Phys 8(3):486–489. https://doi.org/10.1016/j.cap.2007.10.042
14. Chai Q, Jiao Y, Yu X (2017) Hydrogels for biomedical applications: their characteristics and the mechanisms behind them. Gels 3(1):6. https://doi.org/10.3390/gels3010006
15. Jahanban-Esfahlan R, Derakhshankhah H, Haghshenas B, Massoumi B, Abbasian M, Jaymand M (2020) A bio-inspired magnetic natural hydrogel containing gelatin and alginate as a drug delivery system for cancer chemotherapy. Int J Biol Macromol 156:438–445. https://doi.org/10.1016/j.ijbiomac.2020.04.074
16. Lu AH, Salabas EL, Schüth F (2007) Magnetic nanoparticles: synthesis, protection, functionalization, and application. Angew Chem Int Ed 46(8):1222–1244. https://doi.org/10.1002/anie.200602866
17. Liao J, Huang H (2020) Review on magnetic natural polymer constructed hydrogels as vehicles for drug delivery. Biomacromol 21(7):2574–2594. https://doi.org/10.1021/acs.biomac.0c00566
18. Kim C, Kim H, Park H, Lee KY (2019) Controlling the porous structure of alginate ferrogel for anticancer drug delivery under magnetic stimulation. Carbohydr Polym 223:115045. https://doi.org/10.1016/j.carbpol.2019.115045
19. Lakkakula JR, Gujarathi P, Pansare P, Tripathi S (2021) A comprehensive review on alginate-based delivery systems for the delivery of chemotherapeutic agent: doxorubicin. Carbohydr Polym 259:117696. https://doi.org/10.1016/j.carbpol.2021.117696
20. Supramaniam J, Adnan R, Kaus NHM, Bushra R (2018) Magnetic nanocellulose alginate hydrogel beads as potential drug delivery system. Int J Biol Macromol 118:640–648. https://doi.org/10.1016/j.ijbiomac.2018.06.043
21. Ko ES, Kim C, Choi Y, Lee KY (2020) 3D printing of self-healing ferrogel prepared from glycol chitosan, oxidized hyaluronate, and iron oxide nanoparticles. Carbohydr Polym 245:116496. https://doi.org/10.1016/j.carbpol.2020.116496

22. Jafari H, Atlasi Z, Mahdavinia GR, Hadifar S, Sabzi M (2021) Magnetic κ-carrageenan/chitosan/montmorillonite nanocomposite hydrogels with controlled sunitinib release. Mater Sci Eng C 124:112042. https://doi.org/10.1016/j.msec.2021.112042
23. Gambin B, Melnikova P, Kruglenko E, Strzałkowski R, Krajewski M (2022) Impact of the agarose ferrogel fine structure on magnetic heating efficiency. J Magn Magn Mater 550:169000. https://doi.org/10.1016/j.jmmm.2021.169000
24. Omer AM, Sadik WAA, El-Demerdash AGM, Hassan HS (2021) Formulation of pH-sensitive aminated chitosan–gelatin crosslinked hydrogel for oral drug delivery. J Saudi Chem Soc 25(12):101384. https://doi.org/10.1016/j.jscs.2021.101384
25. Samal SK, Goranov V, Dash M, Russo A, Shelyakova T, Graziosi P, Lungaro L, Riminucci A, Uhlarz M, Banobre-Lopez M, Rivas J, Herrmannsdörfer T, Rajadas J, De Smedt S, Braeckmans K, Kaplan DL, Dediu VA (2015) Multilayered magnetic gelatin membrane scaffolds. ACS Appl Mater Interfaces 7(41):23098–23109. https://doi.org/10.1021/acsami.5b06813
26. Siangsanoh C, Ummartyotin S, Sathirakul K, Rojanapanthu P, Treesuppharat W (2018) Fabrication and characterization of triple-responsive composite hydrogel for targeted and controlled drug delivery system. J Mol Liq 256:90–99. https://doi.org/10.1016/j.molliq.2018.02.026
27. Eyadeh MM, Rabaeh KA, Hailat TF, Aldweri FM (2018) Evaluation of ferrous Methylthymol blue gelatin gel dosimeters using nuclear magnetic resonance and optical techniques. Radiat Meas 108:26–33. https://doi.org/10.1016/j.radmeas.2017.11.004
28. Saber-Samandari S, Saber-Samandari S, Joneidi-Yekta H, Mohseni M (2017) Adsorption of anionic and cationic dyes from aqueous solution using gelatin-based magnetic nanocomposite beads comprising carboxylic acid functionalized carbon nanotube. Chem Eng J 308:1133–1144. https://doi.org/10.1016/j.cej.2016.10.017
29. Derakhshankhah H, Jahanban-Esfahlan R, Vandghanooni S, Akbari-Nakhjavani S, Massoumi B, Haghshenas B, Rezaei A, Farnudiyan-Habibi A, Samadian H, Jaymand M (2021) A bio-inspired gelatin-based pH-and thermal-sensitive magnetic hydrogel for in vitro chemo/hyperthermia treatment of breast cancer cells. J Appl Polym Sci 138(24):50578. https://doi.org/10.1002/app.50578
30. Thakur S, Govender PP, Mamo MA, Tamulevicius S, Thakur VK (2017) Recent progress in gelatin hydrogel nanocomposites for water purification and beyond. Vacuum 146:396–408. https://doi.org/10.1016/j.vacuum.2017.05.032
31. Dash R, Foston M, Ragauskas AJ (2013) Improving the mechanical and thermal properties of gelatin hydrogels cross-linked by cellulose nanowhiskers. Carbohydr Polym 91(2):638–645. https://doi.org/10.1016/j.carbpol.2012.08.080
32. Lawrence MB, Joseph J, Usapkar T, Azavedo F (2021) Swelling and DC conductivity behaviour of gelatin-based ferrogels. J Inorg Organomet Polym Mater 31(1):129–137. https://doi.org/10.1007/s10904-020-01682-8
33. Schwabe K, Ewe A, Kohn C, Loth T, Aigner A, Hacker MC, Schulz-Siegmund M (2017) Sustained delivery of siRNA poly-and lipopolyplexes from porous macromer-crosslinked gelatin gels. Int J Pharm 526(1–2):178–187. https://doi.org/10.1016/j.ijpharm.2017.04.065
34. Bhattacharyya SK, Dule M, Paul R, Dash J, Anas M, Mandal TK, Das P, Das NC, Banerjee S (2020) Carbon dot cross-linked gelatin nanocomposite hydrogel for pH-Sensing and pH-responsive drug delivery. ACS Biomater Sci Eng 6(10):5662–5674. https://doi.org/10.1021/acsbiomaterials.0c00982
35. Zhang H, Tian Y, Zhu Z, Xu H, Li X, Zheng D, Sun W (2016) Efficient antitumor effect of co-drug-loaded nanoparticles with gelatin hydrogel by local implantation. Sci Rep 6(1):26546. https://doi.org/10.1038/srep26546
36. Nazeri MT, Javanbakht S, Shaabani A, Ghorbani M (2020) 5-aminopyrazole-conjugated gelatin hydrogel: A controlled 5-fluorouracil delivery system for rectal administration. J Drug Deliv Sci Technol 57:101669. https://doi.org/10.1016/j.jddst.2020.101669
37. Zhang K, Yang J, Sun Y, Wang Y, Liang J, Luo J, Cui W, Deng L, Xu X, Wang B, Zhang H (2022) Gelatin-based composite hydrogels with biomimetic lubrication and sustained drug release. Friction 10:232–246. https://doi.org/10.1007/s40544-020-0437-5
38. Coimbra P, Gil MH, Figueiredo M (2014) Tailoring the properties of gelatin films for drug delivery applications: influence of the chemical cross-linking method. Int J Biol Macromol 70:10–19. https://doi.org/10.1016/j.ijbiomac.2014.06.021
39. Hussain K, Aslam Z, Ullah S, Shah MR (2021) Synthesis of pH responsive, photocrosslinked gelatin-based hydrogel system for control release of ceftriaxone. Chem Phys Lipids 238:105101. https://doi.org/10.1016/j.chemphyslip.2021.105101

40. Özkahraman B, Tamahkar E, İdil N, Kılıç Suloglu A, Perçin I (2021) Evaluation of hyaluronic acid nanoparticle embedded chitosan–gelatin hydrogels for antibiotic release. Drug Dev Res 82(2):241–250. https://doi.org/10.1002/ddr.21747
41. Manish V, Arockiarajan A, Tamadapu G (2021) Influence of water content on the mechanical behavior of gelatin based hydrogels: Synthesis, characterzation, and modeling. Int J Solids Struct 233:111219. https://doi.org/10.1016/j.ijsolstr.2021.111219
42. Ullah K, Khan SA, Murtaza G, Sohail M, Manan A, Afzal A (2019) Gelatin-based hydrogels as potential biomaterials for colonic delivery of oxaliplatin. Int J Pharm 556:236–245. https://doi.org/10.1016/j.ijpharm.2018.12.020
43. Gaihre B, Khil MS, Lee DR, Kim HY (2009) Gelatin-coated magnetic iron oxide nanoparticles as carrier system: drug loading and in vitro drug release study. Int J Pharm 365(1–2):180–189. https://doi.org/10.1016/j.ijpharm.2008.08.020
44. Yakar A, Tansık G, Keskin T, Gündüz U (2013) Tailoring the magnetic behavior of polymeric particles for bioapplications. J Polym Eng 33(3):265–274. https://doi.org/10.1515/polyeng-2012-0034
45. Akin Sahbaz D, Yakar A, Gündüz U (2019) Magnetic Fe_3O_4-chitosan micro-and nanoparticles for wastewater treatment. Part Sci Technol 37:732–740. https://doi.org/10.1080/02726351.2018.1438544
46. Manish V, Siva KV, Arockiarajan A, Tamadapu G (2022) Synthesis and characterization of hard magnetic soft hydrogels. Mater Lett 320:132323. https://doi.org/10.1016/j.matlet.2022.132323
47. Huang Y, Yu H, Xiao C (2007) pH-sensitive cationic guar gum/poly (acrylic acid) polyelectrolyte hydrogels: swelling and in vitro drug release. Carbohydr Polym 69(4):774–783. https://doi.org/10.1016/j.carbpol.2007.02.016
48. Kim SW, Bae YH, Okano T (1992) Hydrogels: swelling, drug loading, and release. Pharm Res 9:283–290. https://doi.org/10.1023/A:1015887213431
49. Nath J, Ahmed A, Saikia P, Chowdhury A, Dolui SK (2020) Acrylic acid grafted gelatin/LDH based biocompatible hydrogel with pH-controllable release of vitamin B_{12}. Appl Clay Sci 190:105569. https://doi.org/10.1016/j.clay.2020.105569
50. Chen X, Fan M, Tan H, Ren B, Yuan G, Jia Y, Li J, Xiong D, Xing X, Niu X, Hu X (2019) Magnetic and self-healing chitosan-alginate hydrogel encapsulated gelatin microspheres via covalent cross-linking for drug delivery. Mater Sci Eng C 101:619–629. https://doi.org/10.1016/j.msec.2019.04.012
51. Zeng N, He L, Jiang L, Shan S, Su H (2022) Synthesis of magnetic/pH dual responsive dextran hydrogels as stimuli-sensitive drug carriers. Carbohydr Res 520:108632. https://doi.org/10.1016/j.carres.2022.108632
52. Li P, Zhou M, Liu H, Lei H, Jian B, Liu R, Li X, Wang Y, Zhou B (2022) Preparation of green magnetic hydrogel from soybean residue cellulose for effective and rapid removal of copper ions from wastewater. J Environ Chem Eng 10(5):108213. https://doi.org/10.1016/j.jece.2022.108213
53. Alinejad-Mir A, Amooey AA, Ghasemi S (2018) Adsorption of direct yellow 12 from aqueous solutions by an iron oxide-gelatin nanoadsorbent; kinetic, isotherm and mechanism analysis. J Clean Prod 170:570–580. https://doi.org/10.1016/j.jclepro.2017.09.101
54. Ji Y, Yang X, Ji Z, Zhu L, Ma N, Chen D, Jia X, Tang J, Cao Y (2020) DFT-calculated IR spectrum amide I, II, and III band contributions of N-methylacetamide fine components. ACS Omega 5(15):8572–8578. https://doi.org/10.1021/acsomega.9b04421
55. Pereira VDA, Ribeiro IS, Paula HC, de Paula RC, Sommer RL, Rodriguez RJS, Abreu FO (2020) Chitosan-based hydrogel for magnetic particle coating. React Funct Polym 146:104431. https://doi.org/10.1016/j.reactfunctpolym.2019.104431
56. Skopinska-Wisniewska J, Tuszynska M, Olewnik-Kruszkowska E (2021) Comparative study of gelatin hydrogels modified by various cross-linking agents. Materials 14(2):396. https://doi.org/10.3390/ma14020396
57. Tanwar A, Date P, Ottoor D (2021) ZnO NPs incorporated gelatin grafted polyacrylamide hydrogel nanocomposite for controlled release of ciprofloxacin. Colloids Interface Sci Commun 42:100413. https://doi.org/10.1016/j.colcom.2021.100413
58. Yin OS, Ahmad I, Amin MCIM (2015) Effect of cellulose nanocrystals content and pH on swelling behaviour of gelatin based hydrogel. Sains Malays 44(6):793–799
59. Yeamsuksawat T, Zhao H, Liang J (2021) Characterization and antimicrobial performance of magnetic Fe_3O_4@Chitosan@Ag nanoparticles synthesized via suspension technique. Mater Today Commun 28:102481. https://doi.org/10.1016/j.mtcomm.2021.102481

60. Rodríguez-Rodríguez R, Espinosa-Andrews H, Velasquillo-Martínez C, García-Carvajal ZY (2020) Composite hydrogels based on gelatin, chitosan and polyvinyl alcohol to biomedical applications: a review. Int J Polym Mater Polym Biomater 69(1):1–20. https://doi.org/10.1080/00914037.2019.1581780
61. Işıklan N, Hussien NA, Türk M (2021) Synthesis and drug delivery performance of gelatin-decorated magnetic graphene oxide nanoplatform. Colloids Surf A Physicochem Eng Asp 616:126256. https://doi.org/10.1016/j.colsurfa.2021.126256
62. Dwivedi R, Singh AK, Dhillon A (2017) pH-responsive drug release from dependal-M loaded polyacrylamide hydrogels. J Sci Adv Mater Dev 2(1):45–50. https://doi.org/10.1016/j.jsamd.2017.02.003
63. Favatela F, Horst MF, Bracone M, Gonzalez J, Alvarez V, Lassalle V (2021) Gelatin/Cellulose nanowhiskers hydrogels intended for the administration of drugs in dental treatments: Study of lidocaine as model case. J Drug Deliv Sci Technol 61:101886. https://doi.org/10.1016/j.jddst.2020.101886
64. Arafa EG, Sabaa MW, Mohamed RR, Elzanaty AM, Abdel-Gawad OF (2022) Preparation of biodegradable sodium alginate/carboxymethylchitosan hydrogels for the slow-release of urea fertilizer and their antimicrobial activity. React Funct Polym 174:105243. https://doi.org/10.1016/j.reactfunctpolym.2022.105243
65. Suhail M, Wu PC, Minhas MU (2021) Development and characterization of pH-sensitive chondroitin sulfate-co-poly (acrylic acid) hydrogels for controlled release of diclofenac sodium. J Saudi Chem Soc 25(4):101212. https://doi.org/10.1016/j.jscs.2021.101212
66. Dangi D, Mattoo M, Kumar V, Sharma P (2022) Synthesis and characterization of galactomannan polymer hydrogel and sustained drug delivery. Carbohydr Polym Technol Appl 4:100230. https://doi.org/10.1016/j.carpta.2022.100230
67. Shariatinia Z, Ziba M (2022) Smart pH-responsive drug release systems based on functionalized chitosan nanocomposite hydrogels. Surf Interfaces 29:101739. https://doi.org/10.1016/j.surfin.2022.101739